

# Supporting Information for: Mechanical Unfolding of Alpha- and Beta-helical Protein Motifs

Elizabeth DeBenedictis<sup>1</sup> and Sinan Keten<sup>1,2,\*</sup>

<sup>1</sup>Department of Mechanical Engineering, Northwestern University, Evanston, Illinois 60208,  
United States

<sup>2</sup>Department of Civil and Environmental Engineering, Northwestern University, Evanston, IL  
60208, United States

\* Corresponding author

E-mail: [s-keten@northwestern.edu](mailto:s-keten@northwestern.edu)

**Figure S1**

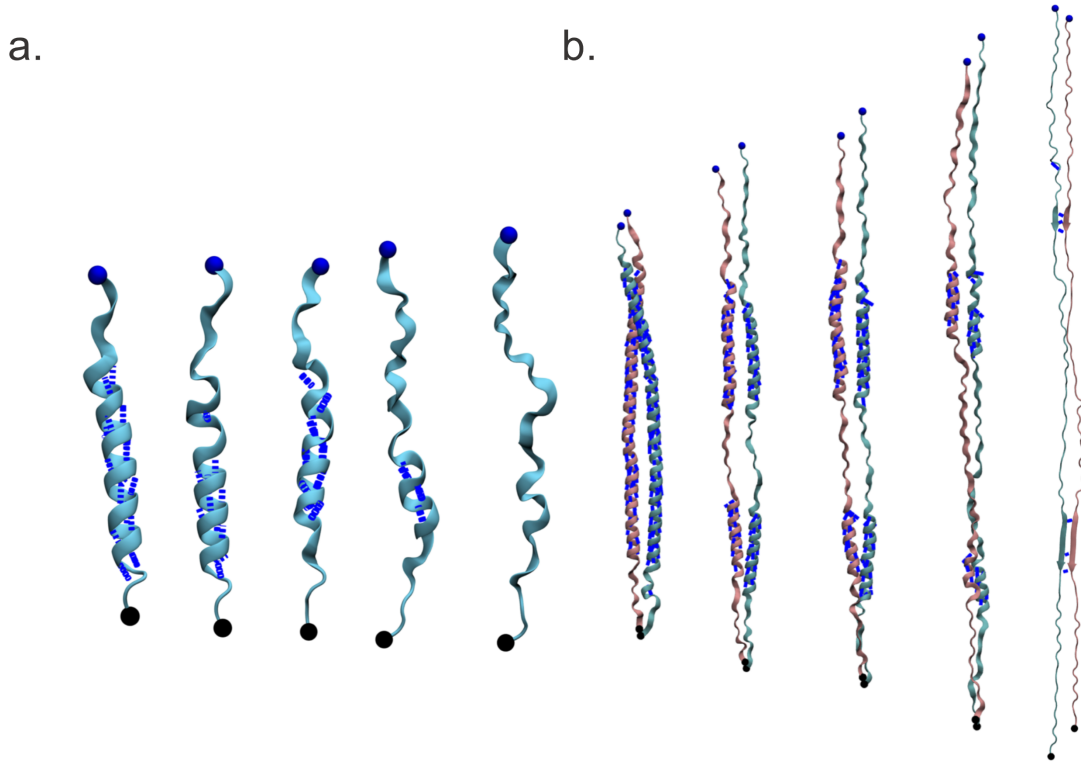


Figure S1: Snapshots of (a) 1coi alpha helix and (b) keratin unfolding. For both alpha-helical proteins, unfolding can initiate at either terminus or in the middle of the helix. During unfolding, helical repeats may reorient, increasing the angle between individual hydrogen bonds and the pulling direction. When fully extended, individual keratin segments form hydrogen bonds together (alpha-beta transition). Snapshots are taken at intervals: 1.7 ns, 2.2 ns, 2.6 ns, 3.6 ns, 4.2 ns for the 1coi alpha helix, and at intervals: 1.5 ns, 7.5 ns, 8.0 ns, 12.5 ns, 17.5 ns for keratin.

**Figure S2**

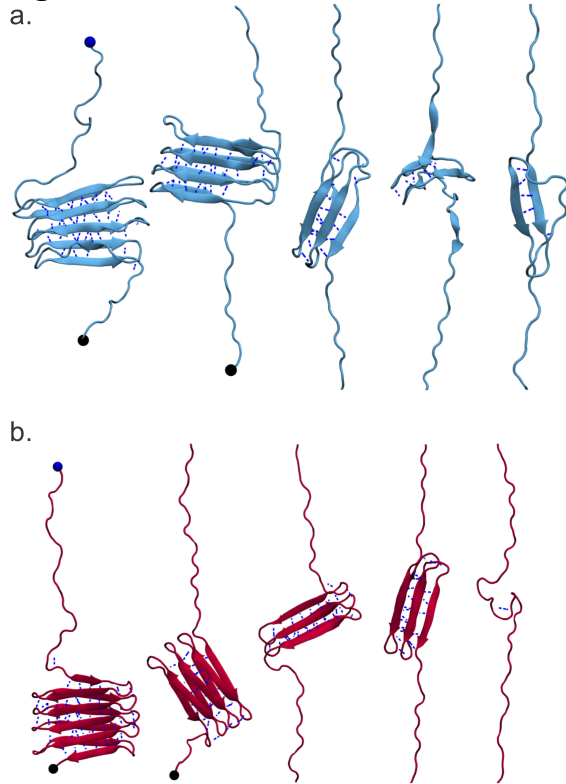


Figure S2: Snapshots of (a) CsgA and (b) CsgB unfolding. During unfolding, the helix core of both CsgA and CsgB proteins reorients to align either pulled end along with the pulling direction. Terminal hydrogen bonds break first and move toward the center of the protein. During reorientation, the helix core can rotate, causing backbone hydrogen bonds to reach near orthogonal angles with the applied force. Snapshots are taken at intervals: 7.1 ns, 14.6 ns, 27.1 ns, 29.5 ns, 34.5 ns for CsgA, and at intervals: 8.2 ns, 17.9 ns, 23.4 ns, 27.5 ns, 38.0 ns for CsgB.

### Single Alpha Helix Unfolding and Size Dependence

In addition to the keratin dimer and the 1coi helix of the coiled coil, single alpha helices from keratin and vimentin were unfolded. This was done using the same simulation conditions as listed in the Methods section, and the PDB IDs used were “1coi” (single helix from coiled coil), “3klt” (vimentin), and “3tnu” (keratin). Visualizations of each protein are shown in Figure S3. One single vimentin helix is shown, although there are four helical segments.

**Figure S3**

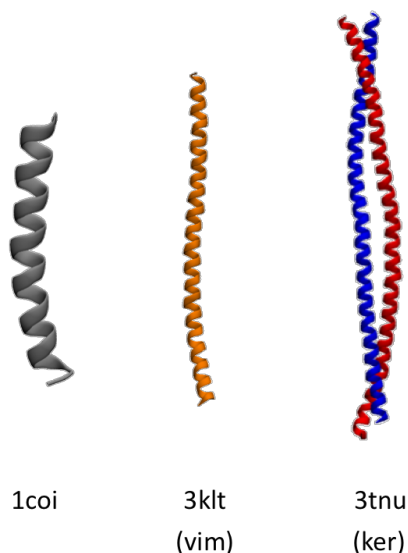


Figure S3. Visualizations of a single alpha-helical peptide from the 1coi coiled coiled coiled, a single vimentin alpha-helix, and the keratin dimer.

For the proteins studied, there is an expected linear increase in work with increasing protein length as shown in Figure S4a. However, even when normalizing the work to unfold by the extended protein length or by number of residues, a trend still exists where longer helices require more work to unfold per unit length (Fig S4b) or per residue (Fig S4c).

**Figure S4**

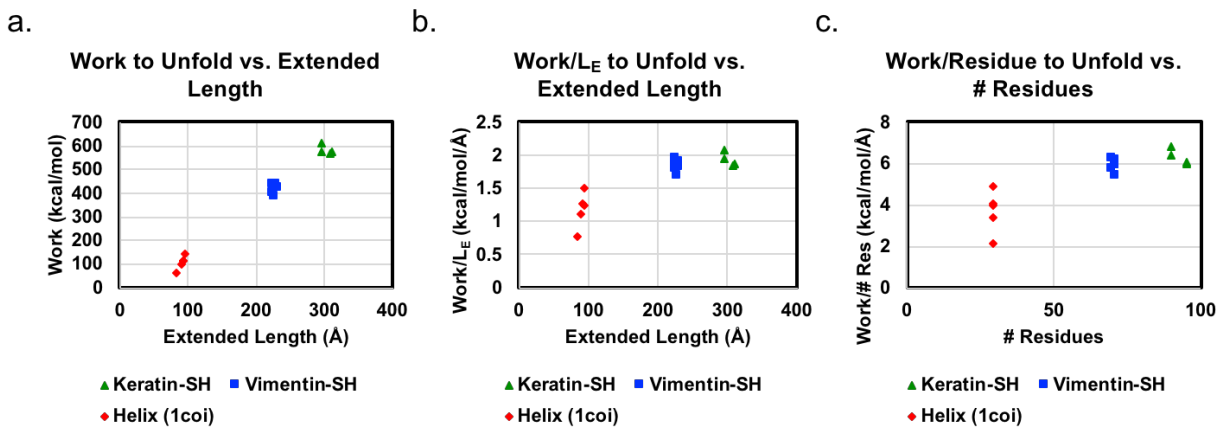


Figure S4. Work (a) and normalized work (b) plotted versus extended length, and normalized work plotted versus number of residues (c) for single alpha-helices.

To investigate cooperative effects of coiled alpha helices during unfolding, we compare the dimer keratin helices with single keratin helices. If the work to unfold both helices as a dimer assembly is equivalent to the sum of each helix alone, this would indicate that no synergistic effect occurs to help resist unfolding. However, if the work to unfold both helices together is

larger than the sum of the parts, keratin dimers may utilize cooperative resistance against unfolding. Because the defined end of unfolding in this study occurs before hydrogen bonds can occur across adjacent helix segments, the alpha-beta transition is not considered, and the expected synergistic effects would be reduced. Indeed, the sum of both keratin segments in all possible combinations resulted in total work values in two trials that were higher than the lowest work trial of unfolding keratin dimers. All other dimer trials required a work to unfold higher than all summed single helix trials. This indicates that even without the alpha-beta transition, slight cooperative effects are seen between adjacent keratin dimers possibly arising from sterically blocking competing water molecules from the backbone.

**Figure S5**

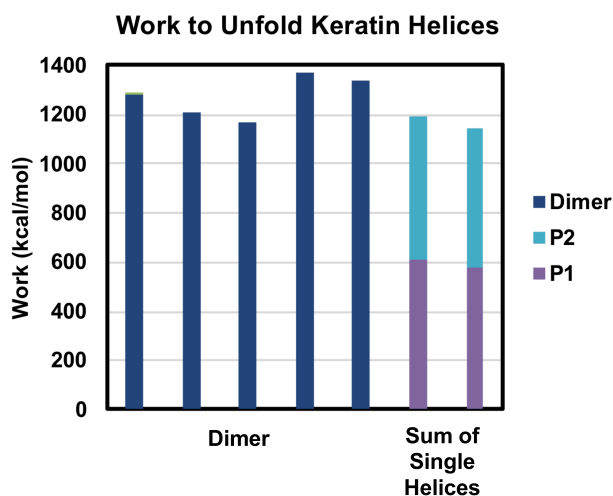


Figure S5. Work to unfold keratin dimers (left) and the total work to unfold both keratin segments independently (right). Only one trial unfolding a keratin dimer (third/middle trial) required less work than any single keratin helix sums.

### Velocity Dependence of Work to Unfold

Explicit unfolding simulations were conducted at additional velocities for CsgA and keratin. The remaining proteins were omitted to minimize computational cost. Three trials at  $v = 2.5$  m/s and 5 m/s were conducted for both CsgA and keratin.

Strain-rate dependence of mechanical unfolding has been oft noted in previous studies, agreeing with our findings. The work to unfold increases with unfolding velocity, as viscous drag forces increase with velocity and fast unfolding rates above the timescale to adequately observe effects from surrounding water molecules and hydrogen bond dynamics will sample stiffer systems<sup>1,2</sup>. Previous studies have found the slope of the rate dependence on unfolding force to vary between different proteins and this slope can be used to obtain the width of the unfolding potential<sup>3</sup>. Also in slower regimes, multiple hydrogen bonds will break concurrently while faster rates will incur hydrogen bond breaking in serial<sup>4</sup>. We see the total work to unfold increase for both CsgA and keratin from 1 to 5 m/s. Linear fits to mean work to unfold at each velocity yield slopes of 740 kcal/mol/m/s for CsgA and 666 kcal/mol/m/s for keratin, indicating differing velocity dependence of work to unfold for both proteins.

**Figure S6**

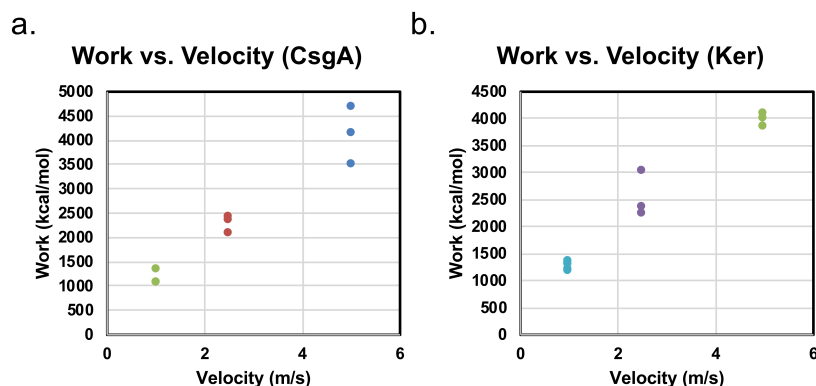


Figure S6. Work vs. Velocity at 1 to 5 m/s for CsgA (a), keratin (b).

### Velocity vs. Strain Rate during Unfolding

Beta-helices can extend to much larger strains than alpha helices due to hidden length within beta-strands. Therefore, at the same velocity, alpha helices are deformed at a higher strain rate than beta-helices. Based on initial lengths, a pulling velocity of 1 nm/ns (1 m/s) yields a strain rate of  $0.4 \text{ ns}^{-1}$  for CsgA and  $0.1 \text{ ns}^{-1}$  for keratin. Keratin achieves a strain rate of  $0.4 \text{ ns}^{-1}$  at a pulling rate of 5 m/s to be comparable with CsgA. In this case, keratin requires over three times the amount of work needed (3977 kcal/mol) to unfold CsgA (1129 kcal/mol) at an equivalent strain rate (1 m/s). At the same strain rate, work to unfold is higher for CsgA when normalized by backbone N-O hydrogen bonds (29.2 kcal/mol/H-bond for keratin, 34.2 kcal/mol/H-bond for CsgA).

### Mechanism Differences – Hydrogen bond Angle

To study the impact of geometry during unfolding, we measure the angle between each backbone hydrogen bond and the pulling direction, as seen in the schematic of Fig S7a. The average angle between each backbone hydrogen bond and the pulling direction over the course of the simulation are plotted versus extension in Fig S7c. Differences in angle pattern are apparent: alpha helices have a gentle increase in angle as increasing hydrogen bonds break and fewer bonds remain that are aligned with the pulling direction, increasing the representation of rotated hydrogen bonds. For beta-helices such as CsgA, several peaks in angle occur with increasing peak height during the simulation. Peaks here represent when the helix core has rotated such that beta-strands are parallel with the pulling direction and the backbone hydrogen bonds are orthogonal to the pulling direction. Peak height increases over the course of the simulation as the helix core height is reduced with each subsequent strand unfolded. Due to these geometric differences, the average backbone hydrogen bond angle throughout the entire simulation is higher for beta-helices than alpha helices. This results in larger displacements required to stretch the hydrogen bond past the breaking point, increasing the work needed to unfold.

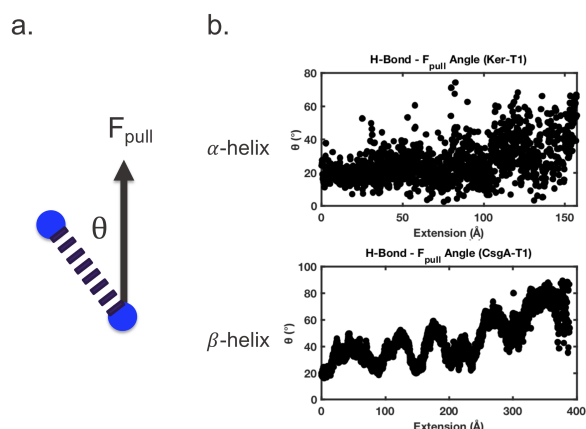


Figure S7. Difference in angle between backbone hydrogen bonds and applied pulling force. Schematic of angle measured (a) and average angle backbone hydrogen bonds and applied pulling force (b).

## References

1. Rief, M.; Pascual, J.; Saraste, M.; Gaub, H. E. J., Single molecule force spectroscopy of spectrin repeats: low unfolding forces in helix bundles, *Journal of Molecular Biology*, **1999**, 286 (2), 553-561.
2. Keten, S.; Alvarado, J. F. R.; Müftü, S.; Buehler, M. J., Nanomechanical characterization of the triple  $\beta$ -helix domain in the cell puncture needle of bacteriophage T4 virus, *Journal of Cellular and Molecular Bioengineering*, **2009**, 2 (1), 66-74.
3. Rief, M.; Gautel, M.; Schemmel, A.; Gaub, H. E. , *Biophysical J.* The mechanical stability of immunoglobulin and fibronectin III domains in the muscle protein titin measured by atomic force microscopy. **1998**, 75 (6), 3008-3014.
4. Ackbarow, T.; Chen, X.; Keten, S.; Buehler, M. J., Hierarchies, multiple energy barriers, and robustness govern the fracture mechanics of  $\alpha$ -helical and  $\beta$ -sheet protein domains. *PNAS*, **2007**, 104 (42), 16410-16415.